

Article

Reducing Rebar Cutting Waste and Rebar Usage of Beams: A Two-Stage Optimization Algorithm

Daniel Darma Widjaja  and Sunkuk Kim * 

Department of Architectural Engineering, Kyung Hee University, Yongin-si 17104, Republic of Korea; danieldarma@khu.ac.kr

* Correspondence: kimsuk@khu.ac.kr; Tel.: +82-31-201-2922

Abstract: While various approaches have been developed to minimize rebar cutting waste, such as optimizing cutting patterns and the lap splice position, reducing rebar usage by minimizing the number of splices remains uninvestigated. In response to these issues, a two-stage optimization algorithm was developed that prioritizes the use of special-length rebar to achieve a near-zero rebar cutting waste (NORCW) of less than 1%, while also reducing overall rebar usage. The two-stage algorithm first optimizes the lap splice position for continuous rebar considering the use of a special-length rebar, which reduces the number of splices required. It then integrates a special-length minimization algorithm to combine the additional rebar. The algorithm was applied to beam structures in a small-sized factory building project, and it resulted in a notable reduction of 29.624 tons of rebar, equivalent to 12.31% of the total purchased quantity. Greenhouse gas emissions were reduced by 102.68 tons, and associated costs decreased by USD 30,256. A rebar cutting waste of 0.93%, which is near zero, was achieved. These findings highlight the significant potential of the proposed algorithm for reducing rebar waste and facilitating sustainable construction practices. The algorithm is also applicable to other reinforced concrete projects, where the associated advantages will be amplified accordingly.

Keywords: rebar cutting waste; rebar usage; lap splice; cutting pattern; two-stage algorithm; optimization



Citation: Widjaja, D.D.; Kim, S.

Reducing Rebar Cutting Waste and Rebar Usage of Beams: A Two-Stage Optimization Algorithm. *Buildings* **2023**, *13*, 2279. <https://doi.org/10.3390/buildings13092279>

Academic Editors: Huihua Chen, Yange Li and Lei Li

Received: 16 July 2023

Revised: 1 September 2023

Accepted: 5 September 2023

Published: 7 September 2023



Copyright: © 2023 by the authors. Licensee MDPI, Basel, Switzerland. This article is an open access article distributed under the terms and conditions of the Creative Commons Attribution (CC BY) license (<https://creativecommons.org/licenses/by/4.0/>).

1. Introduction

The use of concrete and rebar is responsible for 65% of construction-related greenhouse gas emissions, with rebar contributing approximately 60% of the carbon dioxide (CO₂) [1]. Clark and Bradley discovered that rebar generate 872 kg ECO₂/ton of embodied carbon dioxide (ECO₂), whereas C25/30 concrete emits a comparatively lower amount of 95 kg ECO₂/ton [2]. These discoveries emphasize the significant environmental impact posed by rebar worldwide. The Korea Institute of Construction Technology (KICT) [3] defines in their report that the unit CO₂ emissions of high-tensile deformed rebar is 3.466-ton-CO₂/ton. In response to the massive amount of greenhouse gases that are emitted into the atmosphere, many countries have imposed carbon pricing policies. Following a report issued by the CDP in 2021 [4], the carbon price for the construction industry was set at USD 35/ton-CO₂, whereas the Construction Association of Korea [5] notes in their report that the price of rebar in 2022 was USD 900/ton.

Rapid population growth and urban construction have led to a significant increase in construction waste, dominated by concrete and brick waste [6]. Studies from various regions, including New Zealand, Peru, and Hong Kong, have highlighted that metal waste also constitutes a significant proportion of construction waste, encompassing materials such as rebar [7–9]. While concrete and bricks can be recycled or reused, rebar is more challenging to reuse. In the construction of reinforced concrete structures, the generation of rebar cutting waste is an inevitable consequence as the rebar is not manufactured precisely

according to the design [10,11]. In the planning stage, the rebar cutting waste is estimated to be 3–5%; however, construction sites have unexpectedly experienced a higher rebar cutting waste range of 5–8% [10,12,13]. This has resulted in a staggering global rebar cutting waste estimate of 47 million tons, emitting approximately 16 million tons of greenhouse gases in 2019 [10]. Incorporating the previously mentioned carbon price and rebar price, the potential savings in minimizing global rebar cutting waste could amount to a substantial USD 43 billion. In addition, global rebar consumption has been estimated to reach a record of 947 million tons [10]. Reducing steel material at its source is the most effective strategy for reducing carbon emissions and one of the key objectives of implementing sustainable construction practices [14,15]. Consequently, it is crucial to optimize rebar cutting waste and rebar usage, which will substantially reduce the carbon footprint and construction costs. Nevertheless, the effort of minimizing rebar usage remains unexplored.

Numerous studies have been conducted on the optimization of rebar cutting waste have been conducted. Most studies emphasize the utilization of market length to make a combination that diminishes the cutting waste [12,14,16–18]; however, the cutting waste generated utilizing this approach remains notably high. Porwal and Hewage [19] introduced the concept of the special-length combination to optimize rebar cutting waste and obtain favorable outcomes. In addition, several other studies have been conducted to investigate the efficacy of special-length rebar and demonstrate its advantages over market-length rebar [3,19–22]. Nonetheless, the specific constraints for optimization as well as the details of the algorithm operation have not been clearly defined.

The available research of rebar lap splice position optimization offers valuable knowledge regarding the minimization of rebar cutting waste alongside the previously mentioned approaches [12,14,23]. Building design codes suggest that rebar is lapped in the allowable interval area or zones with minimum stress [12]. These studies [12,14,23] mostly comply with the lapping zone regulation provided by building codes. The adoption of the lapping zone inhibits the reduction in rebar cutting waste, resulting in the generation of noticeably high levels of cutting waste. A recent study conducted by Widjaja et al. [24] revealed that the effectiveness of a rebar lap splice is not dependent on the moment force. Furthermore, the study discovered that lap splicing beyond the designated area is structurally sound, providing an essential foundation for devising the proposed algorithm. In a separate study, Almeida et al. [25] asserted that the effectiveness of lap splices relies on several key factors not related to moments; thus, the adjustment made to the lap splice position can be considered acceptable.

1.1. Related Works

Steelworks manufacture and supply special-length rebar at the request of clients or consumers, subject to the minimum requirements, including the minimum quantities and pre-order time [13]. Special-length rebar may include irregular values such as 8.1, 9.4, and 10.6 m. In the context of this study, market-length rebar pertains to specific standard lengths of rebar supplied by the steelworks [11], commonly available in 1 m intervals. An example of the rebar combinations utilizing market-length and special-length rebar is shown in Figure 1. For example, if the required length of the rebar in cutting pattern 1 is 10.8 m, the cutting waste produced by the 12 m market length is 1.2 m (10%), whereas cutting pattern *i* produces 0.8 m (6.67%). In contrast, if a special-length rebar of 11.2 m is ordered, cutting pattern 1 generates only 0.4 m (3.6%) of cutting waste, while cutting pattern *i* produces no cutting waste (0%).

Cutting waste minimization has long been considered a one-dimensional cutting stock problem (1D-CSP). The current practice of identifying cutting patterns in a manner to reduce cutting waste entails a tedious and arduous manual comparison of the feasible possibilities observed, based on the engineer's judgment [12,14,23]. Consequently, numerous approaches were proposed to address 1D-CSP problems, with linear programming (LP) and integer programming (IP) being the most prevalent; however, LP might not result in the optimal solution even though it is efficient [23]. Conversely, IP requires a high compu-

tational effort to generate a feasible solution [19]. The circumstances led the researchers to establish an approach that addresses the limitations and delivers a better solution. Heuristic algorithms provide faster and more effective solutions than conventional approaches, such as the genetic algorithm (GA) [26] and simulated annealing (SA) [19].

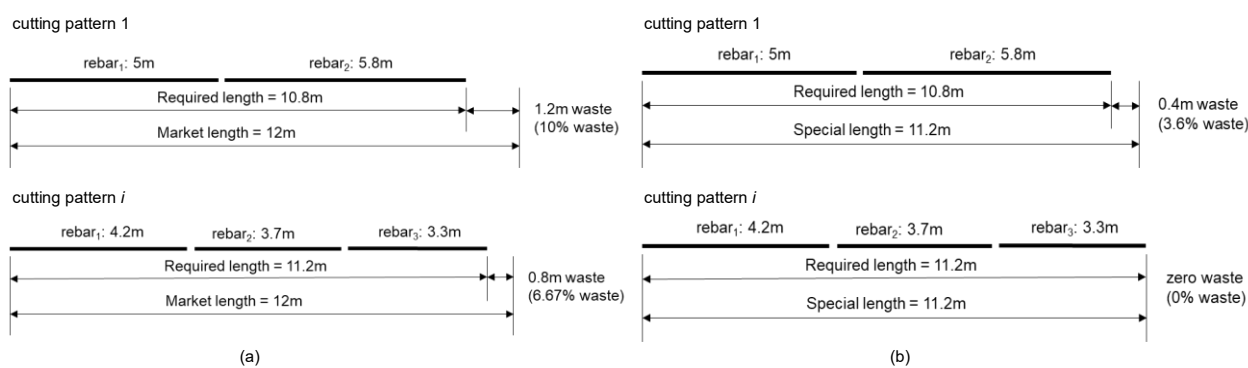


Figure 1. Rebar combinations using market and special-length rebar: (a) combination cases of market-length rebar; (b) combination cases of special-length rebar (adapted from Lee et al. [13]).

Most of the studies conducted have employed market-length rebar to diminish rebar cutting waste. In most cases, the required lengths of rebar during the construction of a project are shorter than the standardized market-length rebar. Consequently, the extraction of required rebar lengths from market-length rebar results in inefficient usage, leading to the generation of rebar cutting waste [11]. Khalifa et al. [26] utilized market-length rebar to reduce the cutting waste in the steelworks, resulting in 5.15% cutting waste. Khondoker [11] employed market-length rebar to reduce rebar cutting waste in RC frames, leading to a rebar cutting waste of 2.69%. Zheng et al. [16] attempted to minimize slab rebar cutting waste by using market-length rebar, resulting in 14.49% cutting waste. Considering the near-zero cutting waste strategy (NORCW), the outcomes obtained in these studies remain noticeably high.

In contrast, Porwal and Hewage [19] introduce the concept of the special-length combination to minimize rebar cutting waste, obtaining 0.93% cutting waste. Kim et al. [22] employed special-length rebar to minimize cutting waste in the bearing wall, resulting in 0.819% cutting waste. In a study performed by Lee et al. [13], special-length rebar was applied to successfully diminish the cutting waste of RC frames to 0.58%. The aforementioned studies confirm that the utilization of special-length rebar offers a lower rebar cutting waste rate than market-length. As cutting waste minimization has been a focus in contributing to sustainable construction practices, there appears to be a lack of attention on minimizing rebar usage as a strategy for fostering sustainability in construction. Considering the enormous global demand for rebar, a reduction in rebar usage would lead to a corresponding reduction in greenhouse gas emissions throughout the project lifecycle.

A different approach was taken by the researchers to minimize the cutting waste by optimizing the lap splice position. The provision of rebar lap joints in RC structures is inevitable due to a variety of reasons, including the limited length of the rebar on-site and transportation problems [27]. The most prevalent types of rebar lap joints employed in construction are welded splices, mechanical splices, and lap splices [28]. Lap splicing or the conventional lap splice requires the overlap of two parallel bars and has been widely recognized as an efficient and cost-effective method of splicing for decades [29].

Building design codes usually specify a permissible interval instead of a single-point zone for the lap splice position [8]. The design code recommends that the zone be situated in an area with minimal stress and moment; however, the construction sites do not strictly adhere to the lapping zone regulations provided by the building codes, which depend on the moment forces. Widjaja et al. [24] discovered that the moment forces do not determine the effectiveness of the rebar lap splice. Gillani et al. [30] inferred that lap splices must have

sufficient length to establish an appropriate bond between the concrete and rebar, ensuring the transfer of force from one bar to another. Almedia et al. [25] furthermore asserted that by providing an appropriate concrete cover, adequate transverse reinforcement confinement, and the high-tensile strength of rebar, the efficacy of lap splicing can be maintained, and lap splice failure can be averted.

In addition, the study conducted by Widjaja et al. [24] provides the following fresh perspectives regarding the lap splice position issue:

1. The provision of lap splices beyond the designated area can offer an equal level of structural strength and stability as those within the designated area;
2. Adhering to the lapping zone regulations provided by the building codes can pose several challenges on construction sites, such as difficulty in identifying the exact location and tedious labor;
3. Several studies that aim for rebar cutting-waste minimization are restricted in their efforts to significantly reduce the cutting waste due to the adherence to the lapping zone regulation.

The adoption of the lapping zone generates noticeably high rebar cutting waste. Chen and Yang [23] attempted to optimize the lap splice position following the ACI code to reduce the rebar cutting waste in a continuous beam section and yielded 8.4% of the cutting waste. Employing the lapping zone provided by the code, Nadoushani et al. [12] attempted to optimize the lap splice position in the columns and shear walls. This effort resulted in 7.2% and 10.6% cutting waste for the columns and shear walls, respectively. Efficient construction practices encourage the placement of lap splices in heavily loaded or high-stressed areas [25,31]. Accordingly, a conventional lap splice could be lapped in the area beyond the designated area subject to the outlined key factors.

The practice of sustainable construction has been encouraged to reduce the impact of the construction industry on the environment, including the issue of rebar cutting waste. The effectiveness of a sustainable design process is contingent upon the integration of both teams to deliver an optimal and least-waste design. Ineffective cooperation, communication, and integration lead to an inefficient, time-consuming, error-prone, and non-sustainable design [19]. BIM enables stakeholders to collaborate during the building design process to efficiently investigate multiple options [19]. BIM involves defining a design as objects that carry geometry, relationships, and attributes that can be extracted to generate useful information [32]. In addition, BIM can be utilized in sustainable analysis to reduce waste and consolidate shipments, thereby reducing carbon footprints even further [33]. Several research studies regarding rebar optimization have integrated BIM to build a structural model and retrieve rebar information [12,19]. Nadoushani et al. [12] utilized a BIM-based database to identify the optimal cutting pattern that produces the least amount of cutting waste. In the early stages of the project lifecycle, Porwal and Hewage [19] incorporated BIM to optimize the rebar waste.

1.2. Objective, Feasibility, and Paper's Structure

Considering the issues presented above, this study proposes a novel heuristic two-stage optimization algorithm for reducing rebar cutting waste and rebar usage of beam elements, realizing the near-zero waste strategy (NORCW) by utilizing the flexibility of the lap splice position and implementing sustainable construction. Beams and columns are the most fundamental and commonly used structural element types in a typical structural RC frame, as they support most of the building's loads [34]. Beam elements are rather more complicated to handle than other structural elements due to the many options regarding reinforcement placement [23]. Moreover, the proposed algorithm has the potential to reduce rebar cutting waste by more than 50% and reduce rebar usage by more than 10% compared to the original design.

The feasibility of this study has been demonstrated by the findings of previous studies [24]. This study has shown that the adjustment of the lap splice position is acceptable. This is a pilot study to reduce rebar cutting waste and rebar usage using a combination

of these innovative concepts: the flexibility of the lap splice position, the reduction in the number of splices, and the use of special-length rebar. The findings of this study could have a significant impact on the construction industry, establish a new paradigm in material waste management, and accelerate the adoption of sustainable construction. This study could have a positive impact on the environment and the economy by reducing rebar cutting waste and rebar usage, which could lead to a reduction in the amount of waste generated in the construction industry and save the industry billions of dollars each year.

The study was carried out and is presented in the following stages. Initially, the problems and originality are defined. Following this, insights and findings from existing studies on the issue of cutting waste are reported, and the heuristic-based two-stage optimization algorithm is then established. Detailed explanations of the market-length and the special-length rebar, rebar minimization, lap splice position, building information modeling, the two-stage optimization process, and algorithms are provided. Furthermore, the rebar cutting waste and rebar usage are investigated in more detail after applying the proposed algorithms to the case study. In addition to rebar cutting waste, the impacts of rebar cutting waste minimization on greenhouse gas emissions and rebar cost reduction are analyzed. Finally, the problems, discoveries, results, and potential for future research are discussed.

2. Methodology

By adjusting the lap splice position, special-length rebar can be generated without cutting; therefore, this study proposes a heuristic approach-based two-stage optimization algorithm to reduce the rebar cutting waste and rebar usage, as well as achieve a near-zero cutting waste strategy (N0RCW) of beams. Two-stage optimization here refers to lap splice optimization and special-length priority optimization. Figure 2 depicts the stages of this study, which are described as follows: 1. model preparation and rebar information collection; 2. the definition of the optimization objective and constraints; 3. the reduction in the number of splices prioritizing special-length rebar without cutting; 4. rebar combination with the cutting pattern; 5. the optimization result analysis considering the rebar cutting waste, rebar usage, greenhouse gas emissions, and associated costs. If a near-zero cutting waste (N0RCW) is achieved, the process is terminated after analyzing the rebar costs and greenhouse gas reduction impact. Otherwise, new parameters must be set, and the optimization process must be conducted again.

Torsion and bending are two critical aspects of external forces to consider in the design of beams. Torsion is the twisting or rotation of a beam caused by twisting forces, which can arise due to eccentric loading or an uneven distribution of the loads. The shear stress flow is related to the distribution of stresses across the cross-section of a beam when it is subjected to torsional loading. Excessive shear stress can cause the beam to fail, compromising its structural integrity. Special torsional reinforcements are embedded in beams to resist the shear stress resulting from torsional loading which is beyond the scope of the present study. When a beam is subjected to a bending moment, normal and shear stresses are developed along its length. The shear stress distribution is crucial in preventing shear failure, which can cause the beam to split along its cross-section. The normal stress distribution ensures that the beam components (concrete and reinforcement) can withstand the compression and tension forces generated due to the bending moment. Longitudinal or main reinforcements are placed along the beam's length to resist bending moments. To resist shear stress, shear or transverse reinforcements are embedded perpendicular to the longitudinal reinforcements in the beam to prevent and control cracks, and to ensure that the beam can withstand the shear loads and deformation without failing. This study primarily focuses on the main rebar of the beams.

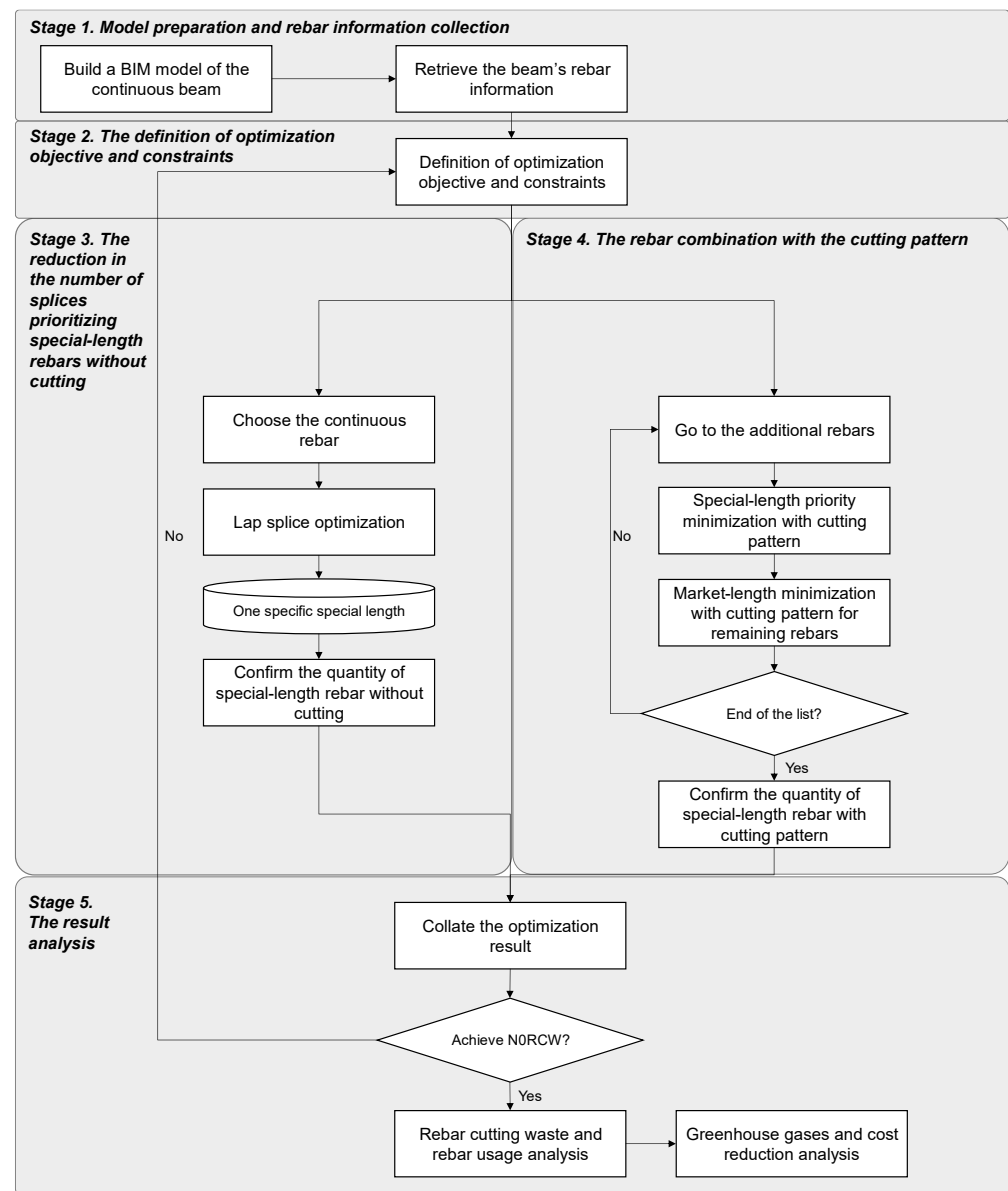


Figure 2. The two-stage optimization algorithm framework.

2.1. Stage 1: Model Preparation and Rebar Information Collection

The structural element is analyzed in this study; the beams were modeled in BIM-based software (Autodesk Revit 2022). Autodesk Revit 2022 was utilized to model the structures according to the dimensions and rebar arrangements of the beam provided by the shop drawing. The usage of rebar details at the shop drawing level is intended not only for dimensional calculation, considering the anchorage, splice location, and length, but also for a precise calculation of the rebar length taking the shape code and bending deduction into consideration. The model developed in Revit includes various important information, including the span length of the beam and the dimension, position, and reinforcement of the structural elements.

The British Standard BS8666:2020 [35] rebar shape code was applied to all the rebar in the Revit model, as shown in Figure 3. The British Standard defines the requirements for the dimensioning, scheduling, cutting, and bending of the rebar. In this study, most of the beams comply with the standard shapes built using the Revit family for the automatic calculation of the rebar lengths. According to the BS code, rebar shapes that do not adhere to the standard code can be classified as shape code 99, which requires the rebar shape

to be drawn with specific dimensions and within the allowed variance. In addition, if there are numerous 99 shape codes, the corresponding rebar sketch must be drawn and alphanumerically appended as 99 (e.g., 99-xxx).

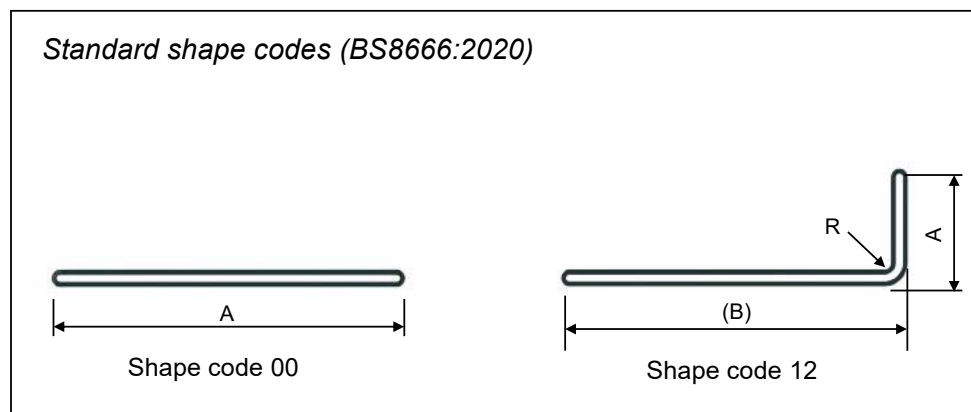


Figure 3. The BS standard shape code for rebar.

BS8666:2020 [35] provides the equations to calculate the length of the rebar, considering the hook and end projection. Table 1 lists the equation used to calculate the length of rebar in the standard shape code. In Figure 3 above, A denotes the rebar's straight and unbent length, while (B) refers to the rebar's straight length before it is bent, and R indicates the minimum radius of bending. Autodesk Revit 2022 can generate a rebar-cutting list that contains the abovementioned information for the optimization processes.

Table 1. Equations of the standard rebar shape codes used.

Standard Shape Code	Equation	Standard Shape Code	Equation
00	A	12	$A + (B) - 0.43R - 1.2d_b$

2.2. Stage 2: The Definition of Optimization Objectives and Constraints

This study seeks to propose a novel two-stage optimization algorithm for optimizing the lap splice position including a reduction in the number of splices in beam elements to realize the near-zero waste strategy (N0RCW), which entails less than 1% of rebar cutting waste and minimizes rebar usage; therefore, constraints are set for special-length rebar as follows: the minimum length is 6 m and the maximum length is 11.9 m, with 0.1 m increments. In addition, the steelwork defines the minimum quantity of rebar required to purchase special-length rebar, and the preorder time. To account for the different requirements of different steelworks, this study defines the minimum purchase quantity of special-length rebar as 50 tons, with a two-month preorder time. The market length available for purchase is 10 m. No minimum order quantity or preorder time is required to purchase market-length rebar, assuming sufficient supply is always maintained.

2.3. Stage 3: The Reduction in the Number of Splices Prioritizing the Special-Length Rebar without Cutting

The lap splice position optimization was then carried out following the retrieval of the rebar information. In addition to lap splice optimization, an approach to reduce the number of splices was also integrated into this stage. The rebar information was arranged in descending order for each rebar diameter size. All the potential lapping arrangements of the main continuous rebar were identified through optimization. Figure 4 illustrates the typical rebar arrangements in the continuous beams system.

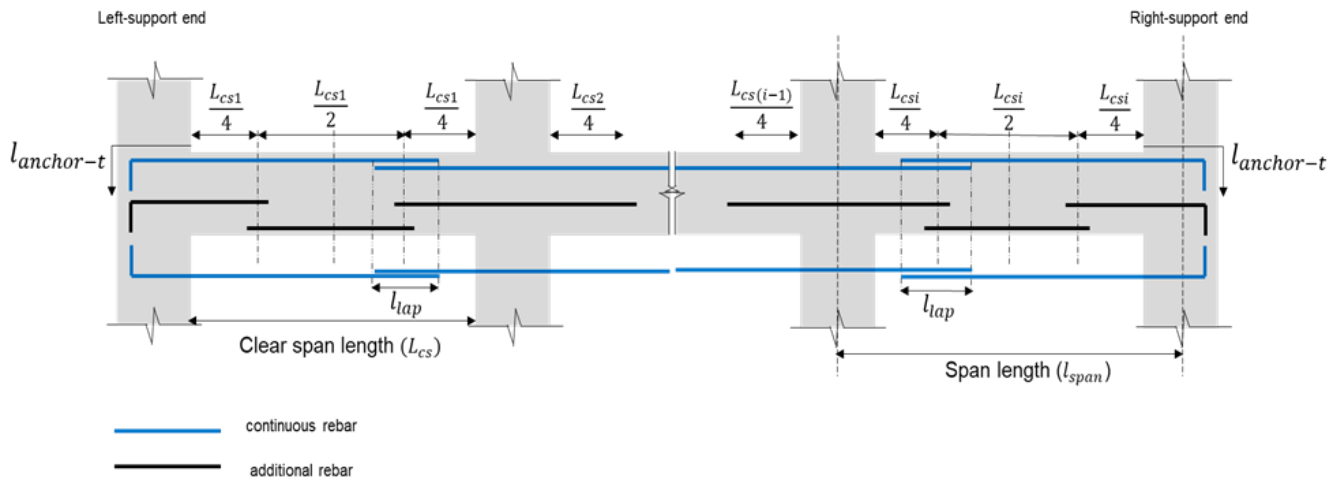


Figure 4. A typical beam rebar arrangement (adapted from Widjaja et al. [36]).

The lapping arrangement in the beam element was identified using Equations (6)–(13) which are proposed in this study. Equations (1) and (2) were provided by the British Standard [37] to determine the tension lap splice length (l_{lap_t}) in the reinforced concrete structures. It was calculated considering the anchorage (development) length of the rebar:

$$l_d = \frac{f_y d_b}{\gamma_m 4 \beta \sqrt{f_{cu}}} \tag{1}$$

$$l_{lap_t} = 1.4 l_d \tag{2}$$

where l_d is the development length (mm), f_y is the yield stress of the rebar (MPa), d_b is the diameter of the rebar (mm), γ_m is the partial safety factor (1.4), β is the coefficient dependent on the rebar type (use a value of 0.5 for tension rebar and 0.63 for compression rebar), and f_{cu} is the compressive strength of concrete (MPa).

As depicted in Figure 5, a continuous beam requires the rebar to be anchored in the column or another beam at both ends. Generally, to anchor, the rebar has to be bent at 90° to create a hook extension height. Equation (3) was used to calculate this hook extension [37]. The total hook anchorage length can be obtained by adding the anchorage length (l_d) and hook extension, as shown in Equation (4), where $l_{anchor-t}$ is the total hook anchorage length (mm) and h_{hook} refers to the hook extension length (mm):

$$h_{hook} \geq 8 d_b \tag{3}$$

$$l_{anchor-t} = l_d + h_{hook} \tag{4}$$

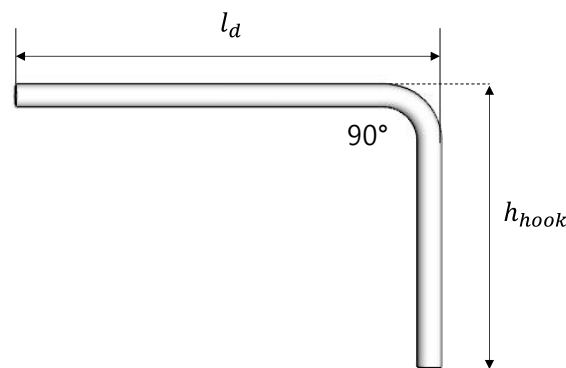


Figure 5. A standard hook anchorage.

The total length of rebar along the continuous beam span (L_{total} ; mm) was calculated as shown in Equation (5) by adding the length of the continuous beam span (l_{span_i} ; mm) with the total hook anchorage length ($l_{anchor-t}$) and total rebar lapping length ($L_{total-lap}$; mm) subtracted by the width of the column at both ends of the beam ($W_l; W_r$; mm) and bending deduction (b_{margin} ; mm) [36]. Equations (6) and (7) were utilized to calculate the total lapping length and bending deduction, respectively [36]:

$$L_{total} = \sum_{i=1}^s l_{span_i} + 2 * l_{anchor-t} + L_{total-lap} - \left(\frac{W_l + W_r}{2} \right) - b_{margin} \quad (5)$$

$$L_{total-lap} = \sum n_{lap} \times l_{lap} \quad (6)$$

$$b_{margin} = 2 \times (0.43R + 1.2d_b) \quad (7)$$

where n_{lap} is the number of laps (pcs), l_{lap} is the lapping length (mm), and R is the minimum bending radius of rebar (mm).

The required number of special length rebar pieces ($n_{special}$; pcs) in Equation (8) was obtained by dividing the total length by the maximum market-length that can be purchased (L_{max} ; mm). In addition, the new number of splices (n_{splice} ; pcs) can be obtained by subtracting one from the number of special length rebar, as illustrated in Equation (9). Furthermore, the difference between the original splice number and the new number of splices denotes the reduction in the number of splices (Δ_{splice} ; pcs), as shown in Equation (10):

$$n_{special} = \text{ceiling} \frac{L_{total}}{L_{max}} \quad (8)$$

$$n_{splice} = n_{special} - 1 \quad (9)$$

$$\Delta_{splice} = n_{lap} - n_{splice} \quad (10)$$

Due to the reduction in the number of splices, the total rebar length should be recalculated. The calculation of the new total rebar length ($L_{n-total}$; mm) is described in Equation (11):

$$L_{n-total} = L_{total} - (\Delta_{splice} \times l_{lap}) \quad (11)$$

As demonstrated in Equation (12), the length of the special-length rebar ($l_{special}$; mm) can be obtained by dividing the new total rebar length by the number of special-length rebar:

$$l_{special} = \text{roundup} \left(\frac{L_{n-total}}{n_{special}} \right) \quad (12)$$

Upon acquiring the length of the special-length rebar, its quantity or weight (Q_{rebar} ; ton) can then be calculated through the multiplication of the length of the special-length rebar by the number of special-length rebar pieces and the unit weight of the rebar (w_{rebar} ; kg/m), as shown in Equation (13):

$$Q_{rebar} = \sum_{i=1}^N l_{special} \times n_{special} \times w_{rebar} \quad (13)$$

The optimization process was conducted in the following steps:

1. After the rebar information was retrieved, the lapping length (l_{lap}) and hook anchorage length ($l_{anchor-t}$) of the rebar was calculated, as described in Equations (1)–(4);
2. The total length of the rebar (L_{total}) was then obtained utilizing Equations (5)–(7);

3. Following this, using Equations (8)–(10), the special-length rebar number ($n_{special}$), the new number of splices (n_{splice}), and the reduction in the number of splices (Δ_{splice}) were calculated;
4. The new total length of the rebar ($L_{n-total}$) was calculated using Equation (11) is calculated;
5. The length of the special-length rebar ($l_{special}$) was determined, which satisfies Equations (9) and (12);
6. After determining the special-length rebar, the rebar lap length was adjusted as required, then the adjusted lap splice arrangement was verified.

2.4. Stage 4: The Rebar Combination with the Cutting Pattern

1. Special-length priority minimization (SLP)

In this stage, special-length priority optimization was performed utilizing special-length rebar to fulfill the objective function defined in Equation (17), as developed in previous studies [13,22]. This stage focuses on the optimization of additional rebar of the beam to identify the best combination; however, before the optimization process can begin, the precise calculation of the additional rebar length should take precedence, as mentioned in Stage 1.

In designing the reinforcement, including the main reinforcement of the structural elements, several factors are taken into consideration, such as the design loads, structural analysis, construction joints, architectural requirements, etc. These factors can result in different rebar arrangements in each beam span, resulting in the requirement that not all rebar is required to be continuously reinforced. This can lead to short and discontinuous rebar pieces, which are also referred to as additional rebar in this study. Short and discontinuous rebar is governed by building codes, such as the ACI 318-14 [38]. This code requires the extension of reinforcement of a distance d (effective depth of the beam; mm) or $12d_b$, beyond the point at which it is calculated to be no longer be required to resist flexure, which is called the additional embedded length. The additional embedded length is either d or $12d_b$, whichever is larger.

As depicted in Figure 4 above, additional rebar can be divided into two groups, additional top rebar and additional bottom rebar. Additional top rebar itself themselves can be distinguished into two categories: additional top rebar for the end support and additional top rebar for the mid support. The previous study introduced a precise calculation approach, presented in Equations (14)–(16), for accurately calculating the length of additional rebar [36]. The additional top rebar for both end supports (L ; mm) can be calculated using Equation (14) considering the hook anchorage length ($l_{anchor-t}$), the beam's clear span length (L_{csi} ; mm), the additional embedded length (l_a ; mm), the column width at either the left or right-support end (W_i ; mm), and the rebar bending deduction (b_{margin}):

$$L = l_{anchor-t} + \left(\frac{L_{csi}}{4}\right) + l_a - W_i - b_{margin} \quad (14)$$

The additional top rebar for the mid-support length (L ; mm) can be obtained considering the beam's clear span length (L_{csi} ; mm), the additional embedded length (l_a ; mm), and the column width at the mid-support end (W_{i+1} ; mm), as shown in Equation (14). If there is a discrepancy in the required number of rebar pieces for the additional top rebar for the mid-support, the smaller number will be prioritized. The remaining rebar will be allocated as additional top rebar for either the left-mid or right-mid position. The length of the relevant rebar pieces can be obtained by using Equation (15) by assigning the (W_{i+1}) and ($L_{cs\ i+1}$) as zero:

$$L = \left(\frac{L_{csi}}{4}\right) + W_{i+1} + \left(\frac{L_{cs\ i+1}}{4}\right) + 2 \times l_a \quad (15)$$

The additional bottom rebar for the middle span (L ; mm) can be acquired utilizing Equation (16) considering the beam's clear span length (L_{csi} ; mm) and additional embedded length (l_a ; mm):

$$L = \left(\frac{L_{csi}}{2} \right) + 2 \times l_a \quad (16)$$

The objective function is fulfilled by minimizing the ratio of cutting waste generated by the special-length rebar (lsp_i); therefore, the optimization was employed to search for the most optimum special-length rebar that satisfies the constraints outlined in Equations (18)–(23) developed in previous studies [13,22], hence reducing the rebar-cutting waste:

$$\text{Minimize } f(X_i) = \sum_{i=1}^N \frac{lsp_i n_i - l_i n_i}{lsp_i n_i} \quad (17)$$

where lsp_i is the special-length i (mm), l_i is the length of the cutting pattern i acquired by combining multiple demand lengths (mm), and n_i is the number of rebar combinations with the same cutting pattern (pcs).

The constraints that must be satisfied to fulfill the objective function are described by Equations (18)–(23). First, the length of cutting pattern i (l_i) is derived by combining multiple demanded rebar pieces, which must be equal to or less than the special-length rebar (lsp_i), as indicated in Equation (18):

$$\text{Subject to } l_i \leq lsp_i, \quad l_i = r_1 + r_2 + \dots + r_n \quad (18)$$

Equation (19) limits the length of special-length rebar (lsp_i) to be longer than the minimum length of the rebar (L_{min} ; mm) and cannot exceed the maximum length of the rebar to be purchased (L_{max} ; mm):

$$L_{min} \leq lsp_i \leq L_{max}, \quad (19)$$

According to Equation (20), the rebar cutting waste (λ) needs to be less than the target rebar cutting waste (λ_t):

$$\lambda = \frac{lsp_i - l_i}{lsp_i} \leq \lambda_t, \quad (20)$$

Subsequently, the total combined special-length rebar quantity (Q_{total} ; ton) must exceed the minimum quantity of special-length rebar to be purchased (Q_{sp} ; ton), as specified in Equation (21):

$$Q_{sp} \leq Q_{total}, \quad 0 \quad (21)$$

Finally, Equation (22) addresses the negativity issue which preventing the proposed algorithm from finding the optimal solution, therefore, this study restricted the number of rebar combinations with the same pattern i (n_i ; pcs) to an integer value:

$$n_i < n_i, \text{ integer}, \quad i = 1, 2, \dots, N \quad (22)$$

2. Quantity calculation

After the special length with the cutting pattern are identified, the quantity or weight (Q_{rebar} ; ton) can be obtained using Equation (23):

$$Q_{rebar} = \sum_{i=1}^N lsp_i \times n_{sp} \times w_{rebar} \quad (23)$$

where lsp is the identified special-length rebar (mm), n_{sp} is the number of identified special-length rebar pieces (pcs), and w_{rebar} is the unit weight of the rebar (kg/m). The rebar combination and quantity or weight market-length rebar can be identified using the set of equation developed in the previous study [13].

2.5. Stage 5: The Result Analysis

The quantities generated in the previous stage were further analyzed. If a near-zero cutting waste was achieved (<1%), the process was terminated after analyzing the rebar costs and CO₂ generated. Otherwise, the constraints were modified, and the optimization was conducted again. The cycle was repeated until a near-zero cutting waste (NORCW) was achieved.

The required quantity (Q_{req}) and purchased quantity of rebar (Q_{pur}) were obtained. The required quantity refers to the actual used quantity at the construction site, while the purchased quantity refers to the purchased quantity of rebar that the contractor purchased from the steelworks. Consequently, the overall rebar cutting waste can be obtained by dividing the difference between the required and purchased quantity by the purchased quantity, as described in Equation (24):

$$RCW = \frac{Q_{pur} - Q_{req}}{Q_{pur}} * 100\% \quad (24)$$

Following this, the performance of the optimization algorithm was verified by comparing the cutting waste generated by the proposed algorithm to the actual cutting waste acquired by utilizing the market-length rebar. In addition to RCW, the rebar usage was also compared. These cutting wastes were then converted into greenhouse gas emissions (CO₂) and the associated costs of rebar through the unit CO₂ emissions and carbon pricing, as mentioned in the previous section. By reducing the rebar cutting waste and rebar usage, the associated rebar costs are reduced. In addition, sustainable construction can be achieved through the reduction in greenhouse gas emissions.

3. Case Study and Verification

3.1. Selection of a Case Project

The beams of a reinforced concrete highrise building for a small-sized factory in Korea were utilized to validate the performance of the proposed algorithm. Seismic activity in Korea is relatively low, with typhoons and storms posing a bigger threat. As summarized in Table 2, the building consists of two basement levels and 20 floors above the ground. Furthermore, ultra-high-tensile deformed (UHD) rebar grade 600 was used in this project for rebar larger than 16 mm.

The building is 104 m in length and 92 m in width. Each floor is connected with the RC column frames ranging from 3.8 m to 5.6 m up to the 20th floor. The beams of the case study building have different dimensions and are reinforced differently, as shown in Figure A1 in Appendix A. Figure 6 shows a rebar arrangement of the G12 beam as an example. As illustrated in Figure 6, the main bars are divided into a top and a bottom section. Both the top and bottom sections are reinforced with 22 mm diameter rebar. The number of rebar pieces within the beams is summarized in Table 3. More rebar arrangements for the remaining beams can be found in Figures A2–A8 in Appendix B.

Table 2. The description of the case study project.

Description	Contents
Location	Korea
Building type	Highrise buildings for small-sized factories
Site area	10,720 m ²
Building area	6317 m ²
Total floor area	72,916 m ²
Number of floors	B2-F20
Structure	Reinforced Concrete (RC)
Concrete strength (f_{cu})	27 MPa
Rebar yield strength (f_y)	>D16, $f_y = 600$ MPa

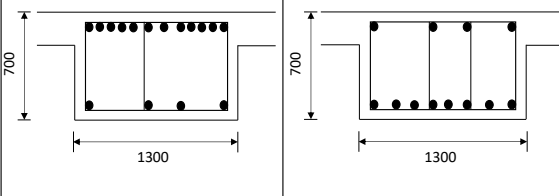
Beam	G12	
Dimension	1300 X 700	
Section	BOTH	CENTER
		
Top	12-UHD22	4-UHD22
Bottom	4-UHD22	8-UHD22
Stirrups	3-HD10@150	4-HD10@300

Figure 6. A sample arrangement for rebar within a beam section.

Table 3. Rebar arrangement within the beams.

Beam	Top				Bottom			
	Left End	Center	Right End	Continuous	Left End	Center	Right End	Continuous
G11A	8	4	12	4	4	8	4	4
G11	14	4	14	4	5	8	5	4
G12	12	4	12	4	4	8	4	4
G13	15	4	15	4	5	10	5	4
G12A	8	4	12	4	4	8	4	4
G6A	7	3	7	3	3	6	3	3
G6	5	3	5	3	3	4	3	3
G26	6	3	6	3	3	5	3	3

3.2. Application of a Two-Stage Optimization Algorithm

In this study, a two-stage optimization algorithm was applied to the longest continuous beam in the short (X) and long (Y) directions. In addition, the proposed algorithm was applied to F2–F7 floors that have similar beam arrangements. As shown in Figure 7, UHD22 mm diameter rebar was used for the main rebar. The optimization procedure was exclusively performed on the main longitudinal rebar. Due to the transversal reinforcements, such as stirrups and ties, which are generally provided in sizes smaller than 16 mm, the utilization of coiled rebar can significantly reduce the rebar cutting waste; thus, the stirrups and ties are excluded from this study.

Initially, the lap splice optimization was performed by prioritizing the special-length rebar and reducing the number of splices, utilizing Equations (6)–(13). Before the optimization, the rebar lapping length (l_{lap}) was recalculated via Equations (1) and (2), aligned with the BS. A partial safety factor (γ_m) of 1.4 and a bond coefficient (β) value of 0.5 were considered for type 2 deformed bars. The concrete compressive strength (f_{cu}) was 27 MPa and the rebar yield strength (f_y) was 600 MPa, hence, the lapping length (l_{lap}) of the UHD22 rebar was 1300 mm for both the bottom and top sections. It is better to design the beam for with both the top and bottom sections in tension to withstand significant lateral forces. In addition, the hook extension height (h_{hook}) was calculated using Equation (4). Since the regulations provided a range for the extension height, a value commonly used in construction sites was selected, resulting in a hook extension height of $12d_b$, or 230 mm for the UHD22 rebar. Subsequently, the length of anchorage ($l_{anchor-t}$) can be calculated using Equation (5). The anchorage length of the UHD22 rebar was 1180 mm. Tables 4 and 5 summarize the beam and rebar information needed, including more detailed beam information.

Table 4. Beam and rebar information.

Description	X-Direction Beam	Y-Direction Beam
Number of spans in relevant direction	7 spans	8 spans
Total length of span ($\sum l_{span}$)	62,700 mm	69,750 mm
Column width at the left support end (W_l)	800 mm	1100 mm
Column width at the right support end (W_r)	1000 mm	1000 mm
Beam depth (D)	700 mm	700 mm
Concrete cover (c)	50 mm	50 mm
Beam effective depth (d)	639 mm	639 mm
Rebar diameter (d_b)	22 mm	22 mm
Lapping/splicing length (l_{lap})	1300 mm	1300 mm
Tension hook anchorage length (l_{anchor_t})	1180 mm	1180 mm
Rebar unit weight (w_{rebar})	2.984 kg/m	2.984 kg/m
Rebar bending deduction (b_{margin})	59.51 mm	59.51 mm

Table 5. Detailed beam information.

Grid	Beam	Span Length (l_{span})	Clear Span Length (L_{cs})	Column Width at the Left Support of a Beam (W_l)	Column Width at the Right Support of a Beam (W_{i+1})
X3-X4	G11A	9300	8500	800	800
X4-X5	G11	9300	8400	800	1000
X5-X6	G12	8400	7400	1000	1000
X6-X7	G12	8400	7400	1000	1000
X7-X8-1	G13	10,200	9200	1000	1000
X8-1-X9-1	G12	8700	7700	1000	1000
X9-1-X11	G12A	8400	7500	1000	800
Y4-Y5	G6A	10,200	9100	1100	1100
Y5-Y6	G6	8550	7700	1100	600
Y6-Y7	G6	8400	7800	600	600
Y7-Y8	G6	8400	7800	600	600
Y8-Y9	G6	8400	7800	600	600
Y9-Y10	G6A	10,200	9400	600	1000
Y10-Y11	G26	7800	6900	1000	800
Y11-Y12	G26	7800	6900	800	1000

The maximum cutting waste was set at 1%. Lap splice optimization was applied in the following constraints: the minimum length of the special-length rebar is 6 m, and the maximum length is 11.9 m, with 0.1 m increments. The minimum quantity (weight) of the special-length rebar was set at 50 tons. The rebar to be optimized was the longitudinal rebar with a 22 mm diameter. The lap splice optimization with the reduction in the number of splices was initially conducted on the continuous rebar; however, the minimum requirement constraint, particularly the minimum quantity, limits the reduction in the rebar cutting waste to higher than 1%. Therefore, the minimum quantity was set to 30 tons, which is lower than the initial 50 tons. Table 6 summarizes the results, providing the special-length rebar without a cutting pattern.

Table 6. Special-length rebar without a cutting pattern.

Diameter (mm)	Special Length (m)	Number of Rebar	Total Quantity (ton)	Purchased Quantity (ton)	Waste Rate (%)
UHD22	11.8	1680	60.130	60.265	0.225
	11.3	1890	64.630	64.925	0.454
Total			124.760	125.190	0.344

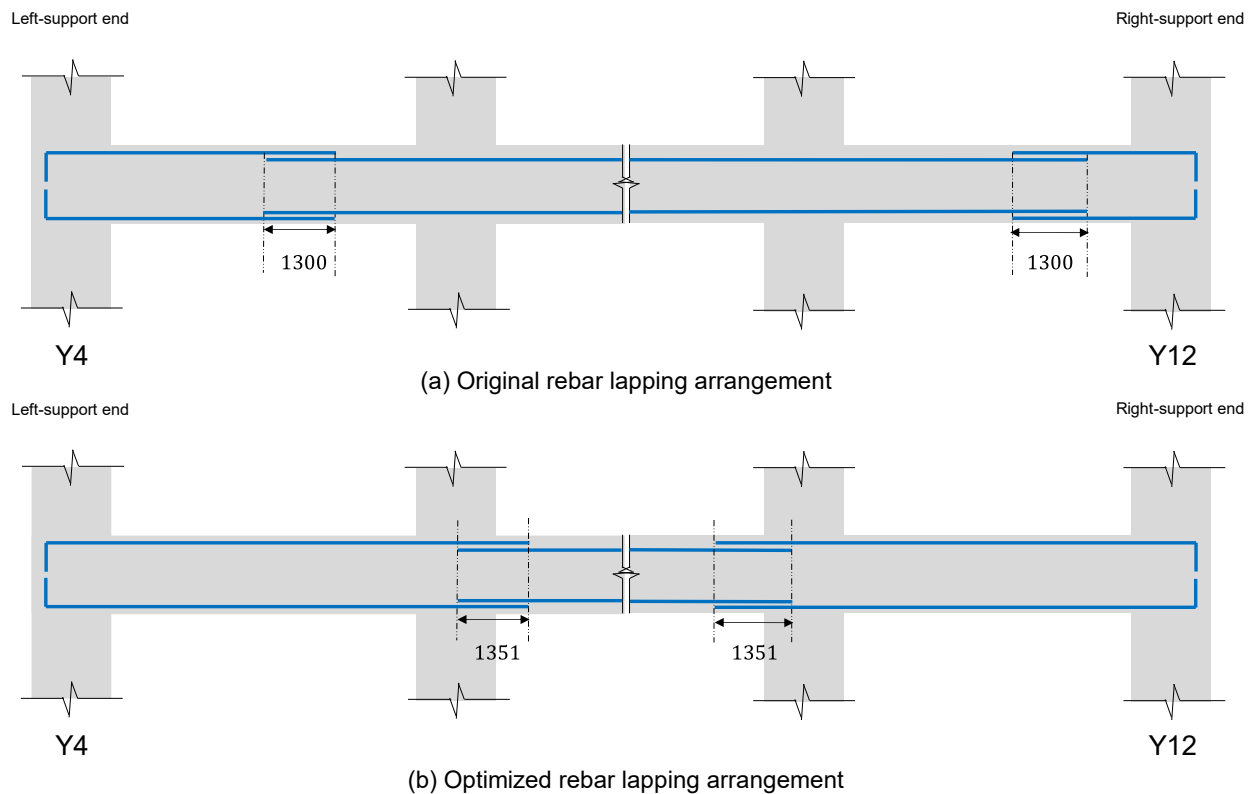


Figure 7. The rebar lapping arrangement: (a) the original rebar lapping arrangement; (b) the optimized rebar lapping arrangement. The blue line indicates the continuous rebars embedded within the beams.

According to Table 6, the special lengths obtained by the proposed algorithm without cutting were 11.8 and 11.3 m. The total quantity required and purchased quantity were 124.760 and 125.190 tons, respectively, with a waste rate of 0.344%. The generated waste rate refers to the loss rate due to the rounding up function imposed, as the special length should be purchased in 0.1 m increments. As no cutting process was involved, the rebar lapping length was adjusted. Figure 7 illustrates the adjustment of the rebar lapping length for beams in the long (Y) direction.

In the following stage, the optimized rebar combination that generated the least amount of rebar cutting waste was obtained by employing Equations (14)–(23). The minimization was conducted on the additional rebar. The constraints set on the special-length rebar in this step were identical to those set in the previous step. The results of the minimization are presented in Table 7.

Table 7. Special-length rebar with cutting patterns.

Diameter (mm)	Special Length (m)	Number of Rebar Pieces	Total Quantity (ton)	Purchased Quantity (ton)	Waste Rate (%)
UHD22	6.6	1575	30.686	31.601	2.90
	11.6	1537	53.577	54.201	1.15
Total			84.263	85.802	1.79%

After minimization, the special-length rebar pieces obtained were 6.6 and 11.6 m in length, as shown in Table 7. The total weight and purchased weight were 84.263 and 85.802 tons, respectively, resulting in a cutting waste of 1.793%. The rebar cutting waste was significantly influenced by the diverse lengths and inherent characteristics of the additional rebar, resulting in a higher rate of rebar cutting waste generation. The total quantity of the special-length rebar purchased in the third and fourth stages exceeded the minimum quantity requirement of 30 tons.

Table 8 details the overall cutting waste rate generated by the proposed algorithm. The total quantity of rebar required for construction was 209.023 tons, and 210.992 tons of special-length rebar had to be purchased. A single diameter of the rebar was used, and a total cutting waste of 0.93% was generated. As shown in Table 8, the utilization of special-length rebar has a significant impact on reducing rebar cutting waste. The special length without cutting accounts for 59.33% of the total rebar, followed by the special length with cutting at 40.67% of the total rebar.

Table 8. A summary of the total rebar-cutting waste.

Description	Waste Rate (%)	Total Quantity (ton)	Purchased Quantity (ton)	Coverage (%)	Cutting Waste (ton)
Special length without cutting	0.34%	124.760	125.190	59.33%	0.430
Special length with cutting	1.79%	84.263	85.802	40.67%	1.539
Total	0.93%	209.023	210.992	100%	1.969

3.3. Verification of the Proposed Algorithm

3.3.1. The Rebar Cutting Waste and Rebar Usage Analysis

A comparative analysis was performed to evaluate the effectiveness of the proposed algorithm by comparing the quantities of rebar in the original and optimized state. The original design of the case study building utilized a market length of 10 m to combine all the required rebar. Table 9 summarizes the comparison result regarding the rebar cutting waste. As shown in Table 9, the original designs and market-length rebar utilization resulted in 27.138 tons of rebar cutting waste, equal to 11.28% of the purchased quantity, whereas the proposed algorithm only generated 1.969 tons or 0.93% of waste. Consequently, this led to a significant reduction of 25.169 tons or 92.75% of the rebar cutting waste.

Table 9. A comparison of original and optimized rebar quantities.

Description	Total Quantity (ton)	Purchased Quantity (ton)	Cutting Waste (ton)	Cutting Waste (%)
Original (O)	213.478	240.616	27.138	11.28
Proposed (P)	209.023	210.992	1.969	0.93
Reduction (O-P)	4.455	29.624	25.169	10.35
Reduction rate (O-P)/O	2.09%	12.31%	92.75%	91.77%

In terms of rebar usage, the original design required the purchase of 240.616 tons of rebar. Conversely, 210.992 tons of rebar should be purchased according to the proposed algorithm, resulting in a reduction of 29.624 tons or 12.31% of rebar. By utilizing special-length rebar, optimizing the lap splice position, and reducing splice numbers, a significant reduction in rebar cutting waste and rebar usage is achieved.

3.3.2. The Constraint Impact

In the previous section, the proposed algorithm was applied with the following constraints in mind: the minimum length of the special-length rebar is 6 m, and the maximum length is 11.9 m, with 0.1 m increments. A minimum quantity (weight) of 50 tons was set for the special length. As mentioned earlier, each steelwork may have its requirements for purchasing rebar of a special length. This section applies the proposed algorithm to the same case study under the following constraints: the maximum rebar cutting waste rate is 1%, the minimum length of the special-length rebar is 6 m, and the maximum length is 11.9 m, with increments of 0.1 m. The minimum quantity (weight) of each diameter and length of the special-length rebar was set at 50 tons; however, this particular set of constraints did not yield any solutions. Hence, the maximum waste rate was increased to 2%. Table 10 outlines the overall rate of cutting waste generated by the proposed algorithm.

The total quantity of rebar required to construct the building was 209.023 tons, and 212.085 tons of special-length rebar had to be purchased. As noted in Table 10, the purchased weight of each special-length rebar exceeds the minimum quantity requirements of 50 tons. The proposed algorithm results in a 1.44% rebar cutting waste. The implication arises from the minimum requirement of 50 tons, indicating that rebar cutting waste exceeding 1% was still generated, thereby resulting in the inability to attain a near-zero cutting waste (NORCW), as previously mentioned. Compared to the previous section, 1.44% of cutting waste was notably higher. This condition indicates that the current constraints, particularly the minimum quantity requirement, affected the performance of the proposed algorithm significantly.

Table 10. The constraint impact on the overall rebar-cutting waste.

Diameter (mm)	Special Length (m)	Number of Rebar Pieces	Total Quantity (ton)	Purchased Quantity (ton)	Waste Rate (%)
Special length without the cutting pattern					
UHD22	11.3	1680	60.130	60.265	0.23%
	11.8	1890	64.631	64.925	0.64%
Total			124.760	125.190	0.44%
Special length with cutting pattern					
UHD22	11.9	2402	84.263	86.895	3.03%
Total			84.263	86.895	3.03%
Overall			209.023	212.085	1.44%

3.3.3. The Effects on Greenhouse Gas (CO₂) Emissions and Cost Reductions

The proposed algorithm was then further analyzed to verify the contribution to sustainable construction. Table 11 provides the greenhouse gas emissions and associated cost reductions after applying the proposed algorithm. In a report published by the Korean Institute of Construction Technology (KICT) [3], the unit CO₂ emissions of high-tensile deformed rebar was reported to be 3.466 ton-CO₂/ton. Incorporating 3.446 ton-CO₂/ton, the greenhouse gas emissions from the original and proposed quantities were 833.98 tons and 731.30 tons, respectively. Consequently, a reduction of 102.68 tons of CO₂ can be achieved; thus, the proposed algorithm has a significant impact on sustainable construction.

Table 11. The effects on greenhouse gas emissions and associated cost reductions.

Description	Quantity (ton)	CO ₂ Quantity (ton)	Rebar Cost (USD)	Carbon Cost (USD)	Total Cost (USD)
Original (O)	240.616	833.98	216,555	29,190	245,745
Proposed (P)	210.992	731.30	189,893	25,596	215,489
Reduction (O-P)	29.624	102.68	26,662	3594	30,256

The associated cost reduction was verified by converting the saved rebar quantity and the CO₂ emissions to a monetary value. In terms of the rebar material costs, the rebar unit price of USD 900/ton published by the Construction Association of Korea [5] was considered, reducing the rebar cost by USD 26,662. In terms of the carbon-associated cost, the carbon price of USD 35/ton-CO₂ provided by the CDP [4] in their report for the construction industry was considered, resulting in a reduction of USD 3594 in the carbon costs. When both cost reductions were tallied, a total savings of USD 30,256 was achieved; therefore, it was confirmed that the proposed algorithm significantly reduces both greenhouse gas emissions and the associated costs, thereby contributing to the implementation of sustainable construction. Greater reductions in greenhouse gas emissions and rebar costs are expected when the proposed algorithm is applied to the entire horizontal structural elements of a building.

4. Discussion

The building code's requirements for the lapping zone often do not consider the conditions and workability of construction sites, resulting in the increased use of rebar and, consequently, higher waste. Furthermore, the authors contend that the lapping zone regulation should be lifted. The author's previous investigation [24] presents a novel perspective suggesting that providing lap splices beyond the designated zone has no impact on structural stability, hence, the proposed algorithm, which does not adhere to the lapping zone regulation, was able to minimize the rebar cutting waste to 0.93%, reaching near zero cutting waste (NORCW).

This study proves that the utilization of special-length rebar can significantly reduce rebar cutting waste and rebar usage. The proposed algorithm was applied to a case study building and successfully reduced the cutting waste by 92.75% and rebar usage by 12.31% compared to the original design. These results are consistent with the expectations stated in the introduction; however, future studies on other types of buildings will be needed to validate these findings. Nonetheless, not all construction professionals are aware of this fact; thus, there is an obstacle to implementing this strategy. Given that only a small number of researchers have attempted to utilize the special length, it is necessary to make greater efforts to encourage its use to achieve sustainable construction more rapidly.

In addition, most steelworks have purchasing requirements for special-length rebar, such as a minimum order of 50 tons and a two-month preorder time. Consequently, the use of special-length rebar is limited to large-scale construction projects. The minimum quantity requirement of 50 tons imposed by steelworks is a trade-off between operational costs and cutting waste. The minimum quantity requirement helps to cover the production, transportation, and storage costs, which ensure stable rebar costs. Nevertheless, the previous section suggests that the minimum quantity requirement may hinder the achievement of a near-zero cutting waste (NORCW), as 1.44% of cutting waste is generated. The minimum quantity policy may cause contractors to over-order rebar, which can lead to waste. If the steelworks can improve accessibility to special-length rebar, for instance by reducing the minimum order quantity and preorder time, this would enable the utilization of special-length rebar in smaller construction projects. Hence, the utilization of special-length rebar is expected to become more prevalent.

Previous studies have predominantly emphasized rebar cutting waste minimization to promote sustainable construction practices; however, there has been noticeably limited

attention on rebar usage minimization. Chen and Yang [23] underscored that the design of the continuous reinforcement should provide as few splices as possible. In this study, the reduction in splice numbers and special-length rebar utilization was proposed to significantly reduce the purchased rebar quantity that will be used in the construction. As a result, a notable reduction of 12.31% in the overall purchased rebar quantity for construction was achieved, highlighting a significant reduction in rebar usage.

Conventional lap splice has been used for decades due to its reliability and cost-effectiveness; however, the lapping length increases proportionately to the rebar diameter. In addition, the lap splice requires a good bond between the spliced rebar to ensure its effectiveness, which requires a longer lap splice length, making it difficult to install and more costly. Furthermore, several building codes prohibit splicing larger diameter rebar, such as the ACI [38], which prohibits splicing rebar larger than 36 mm. Mechanical splices or couplers are used instead of conventional lap splicing to splice these sizes of rebar. Couplers are devices that mechanically connect two adjacent rebar pieces, eliminating the need for lap splicing, and reducing the number of rebar pieces required. They also can be used for rebar with a smaller diameter. The usage of these couplers could further reduce rebar waste and rebar usage, which is a topic that future studies may explore.

5. Conclusions

This study proposes a two-stage optimization algorithm to reduce rebar cutting waste and rebar usage, achieving a near-zero cutting waste strategy (N0RCW). The heuristic-based algorithm was developed according to these two stages: (1) the optimization of the lap splice position for main continuous rebar and reduction in the number of splices to acquire a special length without a cutting pattern; and (2) the special-length priority minimization with the cutting pattern for the additional rebar. This study has identified several important findings that contribute to the effort of minimizing rebar cutting waste and rebar usage, as follows:

1. The proposed algorithm was applied to the beams of a small factory building. The rate of cutting waste for each stage was 0.34% and 1.79%, respectively, resulting in a total cutting waste of 0.93%, hence, a near-zero cutting waste (N0RCW) was achieved;
2. The proposed algorithm reduced the quantity of rebar by 29.624 tons, which is equivalent to 12.31% of the total of the purchased rebar, and reduced 102.68 tons of greenhouse gas emissions and the associated costs by USD 30,256;
3. The results emphasize the lap splice position optimization, splice number reduction, and special-length rebar utilization, which were demonstrated to significantly reduce the rebar cutting waste and rebar usage, contributing to sustainable construction practices;
4. Due to the purchasing requirements for special-length rebar by the steelworks, the proposed algorithm is limited to large-scale construction projects; thus, greater effort is required to encourage the steelworks to simplify the purchasing requirements of special-length rebar, which will contribute to the faster adoption of special-length rebar and the implementation of sustainable construction.

Looking ahead, the authors suggest that future studies should explore the utilization of steel couplers to reduce rebar cutting waste and rebar usage. Couplers connect two adjacent rebar pieces, eliminating the need for the lap splicing method, which could reduce rebar waste and rebar usage in construction projects. Nonetheless, the findings provide a notable framework for reducing rebar cutting waste and rebar usage in the construction industry. Furthermore, the application of the proposed algorithm in construction projects that comprise multiple continuous beam structures will augment the corresponding advantages to a greater extent.

Author Contributions: Conceptualization, S.K.; methodology, D.D.W. and S.K.; validation, S.K.; formal analysis, D.D.W.; investigation, D.D.W.; resources, S.K.; data curation, S.K.; writing—original draft preparation, D.D.W.; writing—review and editing, D.D.W. and S.K.; supervision, S.K.; project

administration, S.K.; funding acquisition, S.K. All authors have read and agreed to the published version of the manuscript.

Funding: This research was supported by the National Research Foundation of Korea (NRF) grant funded by the Republic of Korea government (MOE) (No. 2022R1A2C2005276).

Data Availability Statement: Data sharing is not applicable to this article.

Conflicts of Interest: The authors declare no conflict of interest.

Appendix A

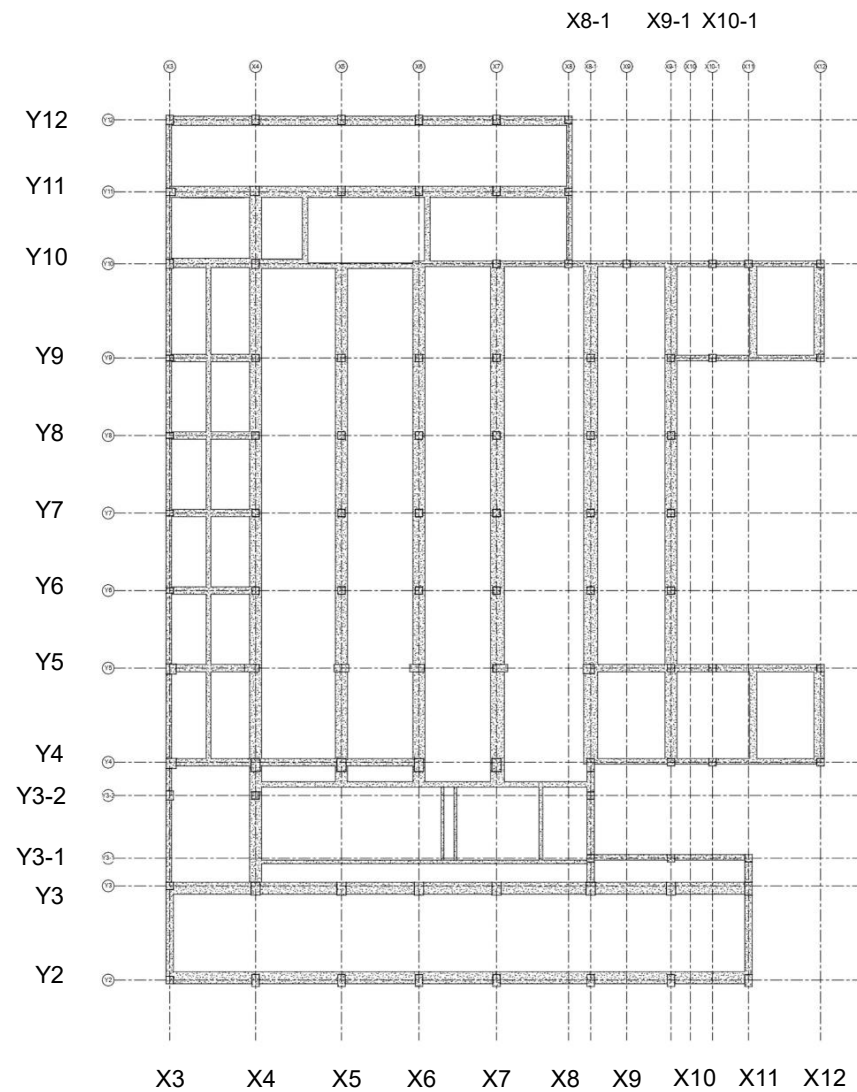


Figure A1. The layout plan of the case study building.

Appendix B

Beam	G6A	
Dimension	600 X 700	
Section	BOTH	CENTER
Top	7-UHD22	3-UHD22
Bottom	3-UHD22	6-UHD22
Stirrups	HD10@150	HD10@300

Figure A2. The rebar details and arrangement for the G6A beam.

Beam	G6	
Dimension	600 X 700	
Section	BOTH	CENTER
Top	5-UHD22	3-UHD22
Bottom	3-UHD22	4-UHD22
Stirrups	HD10@150	HD10@300

Figure A3. The rebar details and arrangement for the G6 beam.

Beam	G11A		
Dimension	1300 X 700		
Section	LEFT-END	CENTER	RIGHT-END
Top	8-UHD22	4-UHD22	12-UHD22
Bottom	4-UHD22	8-UHD22	4-UHD22
Stirrups	3-HD10@150	4-HD10@300	3-HD10@150

Figure A4. The rebar details and arrangement for the G11A beam.

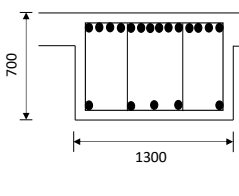
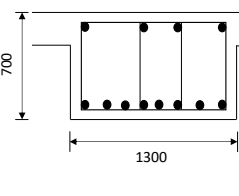
Beam	G11	
Dimension	1300 X 700	
Section	BOTH	CENTER
		
Top	14-UHD22	4-UHD22
Bottom	5-UHD22	8-UHD22
Stirrups	4-HD10@150	4-HD10@300

Figure A5. The rebar details and arrangement for the G11 beam.

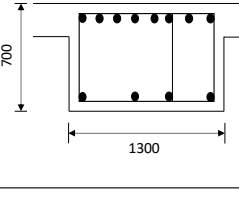
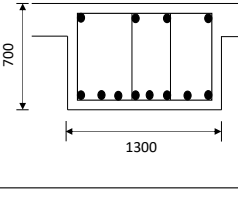
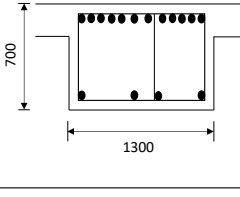
Beam	G12A		
Dimension	1300 X 700		
Section	OUTER-END	CENTER	INNER-END
			
Top	8-UHD22	4-UHD22	12-UHD22
Bottom	4-UHD22	8-UHD22	4-UHD22
Stirrups	3-HD10@150	4-HD10@300	3-HD10@150

Figure A6. The rebar details and arrangement for the G12A beam.

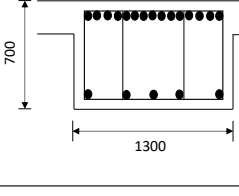
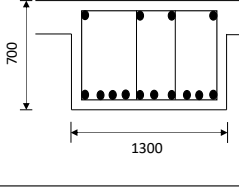
Beam	G13	
Dimension	1300 X 700	
Section	BOTH	CENTER
		
Top	15-UHD22	4-UHD22
Bottom	5-UHD22	10-UHD22
Stirrups	3-HD10@150	4-HD10@300

Figure A7. The rebar details and arrangement for the G13 beam.

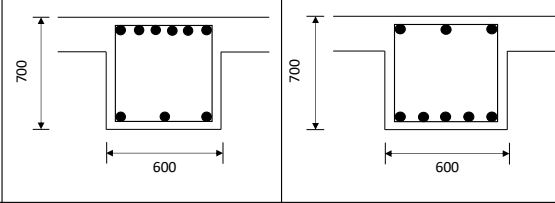
Beam	G26	
Dimension	600 X 700	
Section	BOTH	CENTER
		
Top	6-UHD22	3-UHD22
Bottom	3-UHD22	5-UHD22
Stirrups	HD10@150	HD10@300

Figure A8. The rebar details and arrangement for the G26 beam.

References

- Kim, K.; Jeon, Y.; Park, Y.J.; Park, S. Sustainable Anti-Tank Obstacle System Applying Civil-Military Cooperation in Highly Urbanized Areas. *Sustainability* **2022**, *14*, 12715. [CrossRef]
- Clark, D.; Bradley, D. *Information Paper—31: Embodied Carbon of Steel versus Concrete Buildings*; Cundall Johnston & Partners LLP: Newcastle, UK, 2013; p. 4.
- Korea Institute of Construction Technology (KICT). The Environmental Load Unit Composition and Program Development for LCA of Building: The Second Annual Report of the Construction Technology R&D Program. Korean Institute of Construction Technology, Korea, 2004. Available online: <https://scienceon.kisti.re.kr/srch/selectPORSrchReport.do?cn=TRKO201000018952> (accessed on 17 January 2023).
- CDP. Putting a Price on Carbon. The State of Internal Carbon Pricing by Corporates Globally. Available online: <https://www.cdp.net/en/research/global-reports/putting-a-price-on-carbon> (accessed on 17 January 2023).
- Construction Association of Korea. Construction on Hold as Material Prices Go through the Roof. 2022. Available online: <https://koreajoongangdaily.joins.com/2022/04/22/business/industry/Inflation/20220422165447730.html> (accessed on 17 January 2023).
- Wu, H.; Hu, R.; Yang, D.; Ma, Z. Micro-macro Characterizations of Mortar Containing Construction Waste Fines as Replacement of Cement and Sand: A comparative study. *Constr. Build. Mater.* **2023**, *383*, 131328. [CrossRef]
- Hernandez, G.; Low, J.; Nand, A.; Bu, A.; Wallis, S.L.; Kestle, L.; Berry, T. Quantifying and Managing Plastic Waste Generated from Building Construction in Auckland, New Zealand. *Waste Manag. Res.* **2023**, *41*, 205–213. [CrossRef] [PubMed]
- Rondinel-Oviedo, D.R. Construction and Demolition Waste Management in Developing Countries: A Diagnosis from 265 Construction Sites in the Lima Metropolitan Area. *Int. J. Constr. Manag.* **2023**, *23*, 371–382. [CrossRef]
- Wu, Z.; Yu, A.T.W.; Poon, C.S. An Off-site Snapshot Methodology for Estimating Building Construction Waste Composition—A Case Study of Hong Kong. *Environ. Impact Assess. Rev.* **2019**, *77*, 128–135. [CrossRef]
- Kwon, K.; Kim, D.; Kim, S. Cutting Waste Minimization of Rebar for Sustainable Structural Work: A Systematic Literature Review. *Sustainability* **2021**, *13*, 5929. [CrossRef]
- Khondoker, M.T.H. Automated Reinforcement Trim Waste Optimization in RC Frame Structures using Building Information Modeling and Mixed-Integer Linear Programming. *Autom. Constr.* **2021**, *124*, 103599. [CrossRef]
- Nadoushani, Z.S.M.; Hammad, A.W.; Xiao, J.; Akbarnezhad, A. Minimizing Cutting Wastes of Reinforcing Steel Bars Through Optimizing Lap Splicing within Reinforced Concrete Elements. *Constr. Build. Mater.* **2018**, *185*, 600–608. [CrossRef]
- Lee, D.; Son, S.; Kim, D.; Kim, S. Special-Length-Priority Algorithm to Minimize Reinforcing Bar-Cutting Waste for Sustainable Construction. *Sustainability* **2020**, *12*, 5950. [CrossRef]
- Nadoushani, Z.S.M.; Hammad, A.W.; Akbarnezhad, A. A Framework for Optimizing Lap Splice Positions within Concrete Elements to Minimize Cutting Waste of Steel Bars. In Proceedings of the 33rd International Symposium on Automation and Robotics in Construction (ISARC 2016), Auburn, AL, USA, 21 July 2016. [CrossRef]
- Ma, Z.; Zhao, Q.; Cang, T.; Li, Z.; Zhu, Y.; Hei, X. An Intelligent Optimization Method of Reinforcing Bar Cutting for Construction Site. *Comput. Model. Eng. Sci.* **2023**, *134*, 637–655. [CrossRef]
- Zheng, C.; Lu, M. Optimized Reinforcement Detailing Design for Sustainable Construction: Slab Case Study. *Procedia Eng.* **2016**, *145*, 1478–1485. [CrossRef]
- Zheng, C.; Yi, C.; Lu, M. Integrated Optimization of Rebar Detailing Design and Installation Planning for Waste Reduction and Productivity Improvement. *Autom. Constr.* **2019**, *101*, 32–47. [CrossRef]

18. Zubaidy, S.; Dawood, S.Q.; Khalaf, I.D. Optimal Utilization of Rebar Stock for Cutting Processes in Housing Project. *Int. Adv. Res. J. Sci* **2016**, *3*, 189–193.
19. Porwal, A.; Hewage, K.N. Building Information Modeling–Based Analysis to Minimize Waste Rate of Structural Reinforcement. *J. Constr. Eng. Manag.* **2012**, *138*, 943–954. [[CrossRef](#)]
20. Kim, D.; Lim, C.; Liu, Y.; Kim, S. Automatic Estimation System of Building Frames with Integrated Structural Design Information (AutoES). *Iran. J. Sci. Technol.-Trans. Civ. Eng.* **2020**, *44*, 1145–1157. [[CrossRef](#)]
21. Kim, S.K.; Kim, M.H. A Study on the Development of the Optimization Algorithm to Minimize the Loss of Reinforcement Bars. *J. Archit. Inst. Korea* **1991**, *7*, 385–390.
22. Kim, S.K.; Hong, W.K.; Joo, J.K. Algorithms for Reducing the Waste Rate of Reinforcement Bars. *J. Asian Archit. Build. Eng.* **2004**, *3*, 17–23. [[CrossRef](#)]
23. Chen, Y.H.; Yang, T.K. Lapping Pattern, Stock Length, and Shop Drawing of Beam Reinforcements of an RC Building. *J. Comput. Civ. Eng.* **2015**, *29*, 04014028. [[CrossRef](#)]
24. Widjaja, D.D.; Rachmawati, T.S.N.; Kwon, K.; Kim, S. Investigating Structural Stability and Constructability of Buildings Relative to the Lap Splice Position of Reinforcing Bars. *J. Korea Inst. Build. Constr.* **2023**, *23*, 315–326. [[CrossRef](#)]
25. Almedia, J.P.; Prodan, O.; Tarquini, D.; Beyer, K. Influence of Lap Splices on the Deformation Capacity of RC Walls. I: Database Assembly, Recent Experimental Data, and Findings for Model Development. *J. Struct. Eng.* **2017**, *143*, 04017156. [[CrossRef](#)]
26. Khalifa, Y.; Salem, O.; Shahin, A. Cutting Stock Waste Reduction Using Genetic Algorithms. In Proceedings of the 8th Annual Conference on Genetic and Evolutionary Computation, Seattle, WA, USA, 8–12 July 2006; pp. 1675–1680. [[CrossRef](#)]
27. Dabiri, H.; Kheyroddin, A.; Dall’Asta, A. Splice Methods Used for Reinforcement Steel Bars: A State-of-the-Art Review. *Constr. Build. Mater.* **2022**, *320*, 126198. [[CrossRef](#)]
28. Najafgholipour, M.A.; Dehghan, S.M.; Khani, M.; Heidari, A. The Performance of Lap Splices in RC Beams Under Inelastic Reversed Cyclic Loading. *Structures* **2018**, *15*, 279–291. [[CrossRef](#)]
29. Swami, P.S.; Javheri, S.B.; Mittapalli, D.L.; Kore, P.N. Use of Mechanical Splices for Reinforcing Steel. In Proceedings of the National Conference on Innovative Trends in Engineering and Technology, Solapur, Maharashtra, India, 11–12 March 2016; pp. 1–6. Available online: <https://www.neliti.com/publications/426567/use-of-mechanical-splices-for-reinforcing-steel#cite> (accessed on 17 January 2023).
30. Gillani, A.S.M.; Lee, S.G.; Lee, S.H.; Lee, H.; Hong, K.J. Local Behavior of Lap-Spliced Deformed Rebars in Reinforced Concrete Beams. *Materials* **2021**, *14*, 7186. [[CrossRef](#)] [[PubMed](#)]
31. Haefliger, S.; Kaufmann, W.; Thoma, K. Modelling the Load-Deformation Behaviour of Lap Splices with the Tension Chord Model. *Eng. Struct.* **2022**, *252*, 113606. [[CrossRef](#)]
32. Rajendran, P.; Gomez, C.P. Implementing BIM for Waste Minimisation in the Construction Industry: A Literature Review. In Proceedings of the 2nd International Conference of Management (ICM), Langkawi, Kedah, Malaysia, 11–12 June 2012; pp. 557–570. Available online: https://www.academia.edu/download/34243119/043_191_2ndICM2012_Proceeding_PG0557_0570.pdf (accessed on 17 January 2023).
33. Azhar, S.; Brown, J. BIM for Sustainability Analyses. *Int. J. Constr. Educ. Res.* **2009**, *5*, 276–292. [[CrossRef](#)]
34. Mangal, M.; Cheng, J.C.P. Automated Optimization of Steel Reinforcement in RC Building Frames Using Building Information Modeling and Hybrid Genetic Algorithm. *Autom. Constr.* **2018**, *90*, 39–57. [[CrossRef](#)]
35. British Standard Institute. *Scheduling, Dimensioning, Bending, and Cutting of Steel Reinforcement for Concrete-Specification*, 1st ed.; British Standard Institute: London, UK, 2020; pp. 1–32.
36. Widjaja, D.D.; Kim, D.; Kim, S. Crafting an Automated Algorithm for Estimating the Quantity of Beam Rebar. *J. Korea Inst. Build. Constr.* **2023**, *23*, 485–496. [[CrossRef](#)]
37. British Standard Institute. *Structural Use of Concrete: Code of Practice for Design and Construction-Part 1*, 2nd ed.; British Standard Institute: London, UK, 1997; pp. 1–150.
38. American Concrete Institute. *Building Code Requirements for Structural Concrete and Commentary (Metric)*, 1st ed.; American Concrete Institute: Farmington Hills, MI, USA, 2014; pp. 1–519.

Disclaimer/Publisher’s Note: The statements, opinions and data contained in all publications are solely those of the individual author(s) and contributor(s) and not of MDPI and/or the editor(s). MDPI and/or the editor(s) disclaim responsibility for any injury to people or property resulting from any ideas, methods, instructions or products referred to in the content.